Gas phase infrared spectroscopy of cluster anions as a function of size: The effect of solvation on hydrogen-bonding in $Br^-\cdot(HBr)_{1,2,3}$ clusters

Nicholas L. Pivonka
Department of Chemistry, University of California, Berkeley, California and Chemical Sciences Division, Lawrence Berkeley National Laboratory, Berkeley, California 94720

Cristina Kaposta
Institut für Experimentalphysik, Freie Universität Berlin, Arnimallee 14, D 14195 Berlin, Germany

Gert von Helden
FOM Institute for Plasmaphysics Rijnhuizen, Edisonbaan 14, NL-3439 MN, Nieuwegein, The Netherlands

Gerard Meijer
FOM Institute for Plasmaphysics Rijnhuizen, Edisonbaan 14, NL-3439 MN, Nieuwegein, The Netherlands and Department of Molecular and Laser Physics, University of Nijmegen, Toernooiveld, NL-6525 ED, Nijmegen, The Netherlands

Ludger Wöste
Institut für Experimentalphysik, Freie Universitat Berlin, Arnimallee 14, D 14195 Berlin, Germany

Daniel M. Neumark[a)]
Department of Chemistry, University of California, Berkeley, California and Chemical Sciences Division, Lawrence Berkeley National Laboratory, Berkeley, California 94720

Knut R. Asmis[b)]
Institut für Experimentalphysik, Freie Universität Berlin, Arnimallee 14, D 14195 Berlin, Germany

(Received 24 May 2002; accepted 22 July 2002)

The gas phase vibrational spectroscopy of $Br^-\cdot(HBr)_{1,2,3}$ clusters has been studied between 6 and 16 μm (625 and 1700 cm^{-1}) by multiphoton infrared photodissociation spectroscopy using the output of the free electron laser for infrared experiments. Infrared (IR) spectra were recorded by monitoring the mass-selected ion yield. In all three systems neutral HBr loss is found to be the dominant photofragmentation channel. $BrHBr^-$ exhibits a weak absorption band at 1558 cm^{-1} which is assigned to the overtone of the antisymmetric stretching mode ν_3. A series of strong absorption bands was observed for $Br^-\cdot(HBr)_2$ at energies in the 950–1450 cm^{-1} range. The $Br^-\cdot(HBr)_3$ spectra reveal two absorption bands at 884 and 979 cm^{-1}, which are assigned to two H-atom stretching modes. Evidence for the localization of the H atom and destruction of the symmetric $BrHBr^-$ hydrogen bond in the larger clusters is presented. Standard electronic structure calculations fail to reproduce the experimental IR spectra, indicating a breakdown of the harmonic approximation. © *2002 American Institute of Physics.* [DOI: 10.1063/1.1506308]

I. INTRODUCTION

The hydrogen bond is one of the most important interactions in chemistry, governing diverse phenomena from the properties of liquids to the structure of proteins and DNA.[1] Hydrogen bonds are particularly appealing from the perspective of cluster spectroscopy, which can probe how the properties of a collection of molecules held together by hydrogen bonds evolve with size.[2] Such studies have shown, for example, how many of the properties of liquid water can be understood in terms of fundamental interactions between water molecules.[3]

Some of the strongest known hydrogen bonds are the symmetric bihalide anions XHX^- (X=F, Cl, Br, I), with dissociation energies ranging from 1.93 eV for FHF^- to 0.73 eV for IHI^-.[4] Experiments and calculations indicate these anions to be symmetric, $D_{\infty h}$ species with two equal H–X bond lengths.[5–16] These anions and their asymmetric counterparts, such as $BrHI^-$, are also of interest as transition state precursors in negative ion photoelectron spectroscopy experiments.[17,18] However, the very factor that causes these hydrogen bonds to be so strong, namely the extensive sharing of the H-atom between two halogen atoms, also makes these bonds highly susceptible to solvent perturbation that can, for example, destroy the symmetry of the bonds in symmetric XHX^- anions. In this paper, we use the tunable infrared (IR) radiation from a free electron laser to obtain the first gas phase spectrum of $BrHBr^-$ and probe the effect of solvation on the hydrogen-bonding in this anion via IR spectroscopy of size-selected $Br^-\cdot(HBr)_n$ clusters.

Considerable recent progress has been made in the IR spectroscopy of hydrogen-bonded anion clusters, primarily

a)Author to whom correspondence should be addressed. Electronic mail: dan@radon.cchem.berkeley.edu
b)Author to whom correspondence should be addressed. Electronic mail: asmis@physik.fu-berlin.de

TABLE I. Experimental infrared band positions and intensities.

Parent ion	Fragment ion	Position (cm^{-1}) and normalized intensity
$BrHBr^-$	Br^-	1558
$Br^-\cdot(HBr)_2$	$BrHBr^-$	~875 (0.05), ~940 (0.06), 992 (1.00), 1012 (0.74), 1048 (0.73), 1104 (0.75), 1147 (0.56), 1205 (0.16), 1222 (0.10), 1269 (0.10), 1289 (0.10), 1359 (0.66), 1420 (0.27)
$Br^-\cdot(HBr)_3$	$Br^-\cdot(HBr)_2$	888 (1.00), 979 (0.16)
	$BrHBr^-$	884 (0.07), 934 (0.08), 984 (1.00), 1052 (0.11), 1098 (0.08), 1142 (0.06), 1203 (0.03), 1225 (0.01), 1264 (0.01), 1289 (0.01), 1359 (0.06), 1416 (0.04)

through IR predissociation experiments in which size-selected clusters are vibrationally excited with one or more IR photons, and then predissociate to daughter ions that can be detected with near-unit efficiency.[19–23] This type of IR action spectroscopy is extremely sensitive and can be applied to mass-selected ion beams where number densities are as low as $10^3-10^4/cm^3$. These experiments require intense, tunable laser sources, and have thus been largely restricted to vibrational frequencies above 2350 cm^{-1}. However, for strongly hydrogen-bonded anions such as symmetric bihalides, the antisymmetric stretch (ν_3) fundamental is considerably lower than this; gas phase IR spectroscopy of FHF^- and $ClHCl^-$ yields ν_3 frequencies of 1331 and 723 cm^{-1}, respectively,[10,11] while matrix isolation spectroscopy of $BrHBr^-$ yields ν_3 frequencies ranging from 728 to 753 cm^{-1}.[8,12] Hence, the systematic study of the IR spectroscopy of bare and clustered bihalides requires a very different type of light source.

A novel approach to study the vibrational spectroscopy of cations in the spectral region below 2000 cm^{-1} using infrared photodissociation (IRPD) spectroscopy has recently been demonstrated by Meijer and co-workers using the free electron laser for infrared experiments (FELIX) at the FOM-Institute Rijnhuizen.[24–27] Multiphoton excitation IRPD spectra of selected polycyclic aromatic hydrocarbons were measured using excimer laser ionization followed with multiphoton excitation with a pulsed free electron laser (FEL) in the 400–1700 cm^{-1} region. Asmis *et al.*[28] extended the technique to study mass-selected parent ions by coupling a tandem-mass spectrometer to the FEL source. In the present study, we apply this technique for the first time to investigate the vibrational spectroscopy of gas phase cluster anions. Our results indicate that the addition of one or more HBr solvent molecules to the $BrHBr^-$ cluster destroys the symmetry of the $BrHBr^-$ bond, with the resulting system resembling two or three HBr ligands bound to a Br^- core.

II. EXPERIMENT

$Br^-\cdot(HBr)_n$ clusters are produced at the intersection of a pulsed supersonic molecular beam and a 1 keV, 300 μA electron beam using an arrangement similar to that used in previous photoelectron spectroscopy studies of $BrHBr^-$.[18] The molecular beam is formed from a gas mixture of 4% HBr in Ar, which is expanded through a pulsed valve (General Valve) with a 780 μm diameter orifice. The pulsed valve is operated at 20 Hz with a stagnation pressure of 2–5 bar. Br^- ions are formed through dissociative electron attachment to HBr and are clustered and internally cooled as the supersonic expansion progresses. Anion clusters generated in the supersonic expansion pass a 2 mm skimmer into a previously described guided ion beam tandem mass spectrometer,[28] where they are mass-selected and subsequently trapped in a temperature-adjustable, helium filled radio frequency (RF) hexadecapole ion trap. The ion trap is kept at a constant temperature of ~50 K and He buffer gas pressure of ~80 μbar.

Infrared excitation is performed with the output of FELIX.[29] The FELIX output is composed of 5 μs long macropulses at 5 Hz, with each macropulse containing a series of ~1 ps micropulses separated by a nanosecond. The FELIX bandwidth is transform limited to ~0.8% of the central frequency and pulse energies of 50 and 25 mJ per macropulse (measured before the ZnSe optics) were employed in these experiments. The FELIX beam is directed through two ZnSe windows and focused within the ion trap by a 600 mm focal length ZnSe lens. The scan range for these experiments was limited by the IR transmission function of the ZnSe windows and lenses which was >85% between 8 and 14 μm and dropped to <10% below 6 μm and above 17 μm. When FELIX is in resonance with an infrared transition of the trapped anion, multiple photon absorption and dissociation can occur, leading to production of ionic photofragments, as follows:

$$AB^-(\nu=0)\xrightarrow{h\nu}AB^-(\nu=1)\xrightarrow{nh\nu}A^-+B. \quad (1)$$

During a measurement cycle, the ion trap is allowed to fill for a period of 290 ms and the ions are then stored until a trigger signal from the FEL is received. During this time either two or three FELIX macropulses interact with the trapped ions, producing photofragment ions if multiphoton dissociation occurs. The trap is partially emptied over a period of 100 ms and the mass-selected ion yield is recorded as a function of the FEL wavelength. Depending on the signal intensity, this process is repeated over 5–20 fill/extraction cycles and for each fragment ion monitored. The stability of the parent ion production is checked by measuring the parent ion yield once at the beginning and once at the end of each wavelength step. The ion trap is completely emptied after

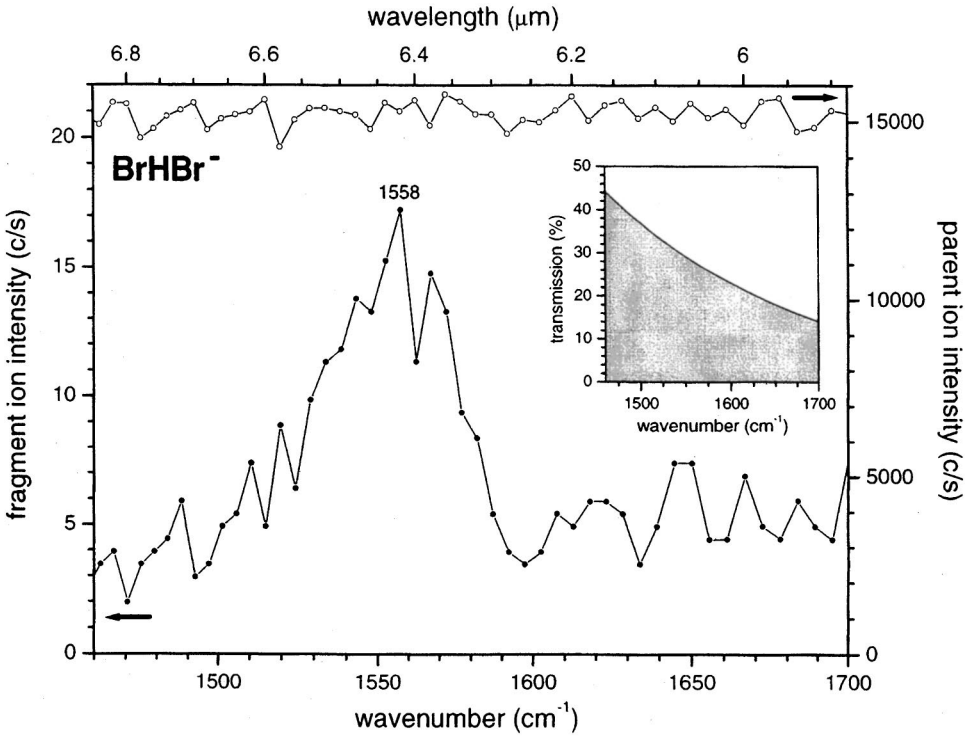

FIG. 1. Parent ion (open dots) and Br^- fragment ion (solid dots) IRPD spectrum of $BrHBr^-$. Inset shows transmission efficiency of ZnSe optics.

each wavelength step. A typical spectrum is measured in steps of 20–100 nm and takes roughly 30–60 min to record. Peak positions are summarized in Table I.

III. RESULTS

A. $BrHBr^-$

The IRPD spectrum of $BrHBr^-$ in the range from 1460 to 1700 cm^{-1} is shown in Fig. 1. Both parent ion (open dots) and Br^- fragment ion (solid dots) intensities are plotted. The parent ion signal, which was measured with less signal averaging than the fragment ion signal, varies by $<10\%$ over the acquisition time. A single broad, weak absorption band is observed in the Br^- fragment ion yield (HBr loss channel) at 1558 cm^{-1} with a full width at half maximum of 60 cm^{-1}. Depletion of the parent ion signal is not resolved, because it is three orders of magnitude smaller than the parent ion signal itself. Coarser scans extending from 625 to 1700 cm^{-1} showed no additional features, nor did finer scans from 700–800 cm^{-1}, where the ν_3 antisymmetric stretch fundamental is expected.[7,8,12,15,16,30] A constant Br^- background signal resulting from collision induced dissociation of the $BrHBr^-$ parent ions is observed. The Br^- background is on the order of 0.03% of the parent ion signal, and photofragmentation at 1558 cm^{-1} yields approximately three times the background signal. The transmission of the ZnSe optics (inset of Fig. 1) strongly decreases below 8 μm and varies by a factor of ~ 3 in the shown spectral region. As a result of this the band shape may be distorted due to the decreasing pulse energy at the interaction region.

B. $Br^-\cdot(HBr)_2$

Figure 2 shows IRPD spectra of $Br^-\cdot(HBr)_2$. The dominant photofragment channel is production of $HBr+BrHBr^-$ (solid dots). The parent ion depletion spectrum is also shown (top right corner). In contrast to $BrHBr^-$, the parent depletion is quite pronounced. At 992 cm^{-1}, the largest absorption band, roughly 85% of the parent ions are depleted, indicating that photofragmentation does not exclusively occur at the focus of IR beam, but extends over the complete irradiated region of the 23 cm long ion trap. Collisional fragmentation of $Br^-\cdot(HBr)_2$ within the ion trap gave a small baseline $BrHBr^-$ signal of ~ 70 c/s over the entire scan range. The depletion and fragment ion spectra exhibit a strong correlation, with six distinct, strong absorption peaks appearing at 992, 1048, 1104, 1147, 1359, and 1420 cm^{-1}. The 992 cm^{-1} feature exhibits a shoulder at 1012 cm^{-1}, hinting at an addi-

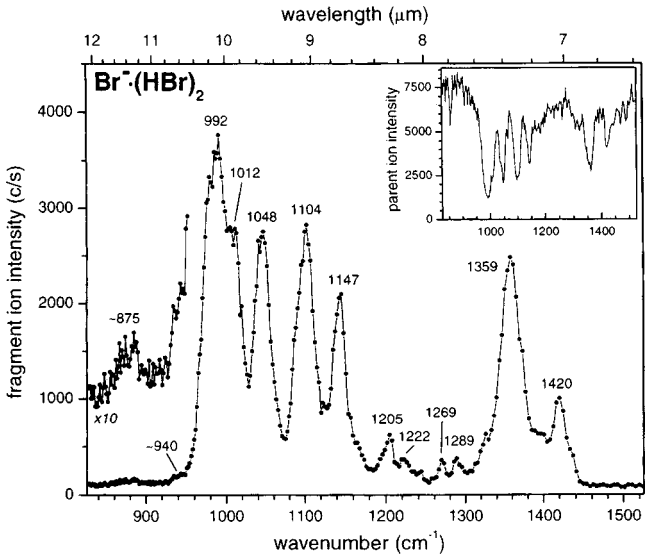

FIG. 2. $BrHBr^-$ fragment ion IRPD spectrum of $Br^-\cdot(HBr)_2$ (solid dots). Inset shows the corresponding $Br^-\cdot(HBr)_2$ parent depletion spectrum.

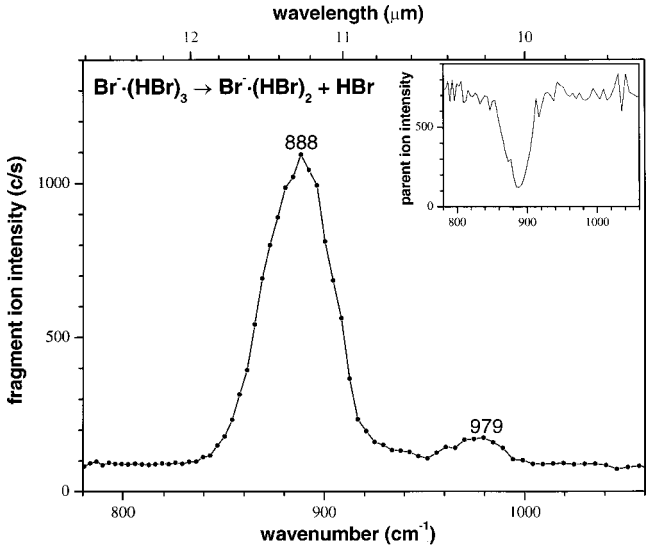

FIG. 3. $Br^-(HBr)_2$ fragment ion IRPD spectrum of $Br^-\cdot(HBr)_3$ (solid dots). Inset shows the corresponding $Br^-(HBr)_3$ parent depletion spectrum.

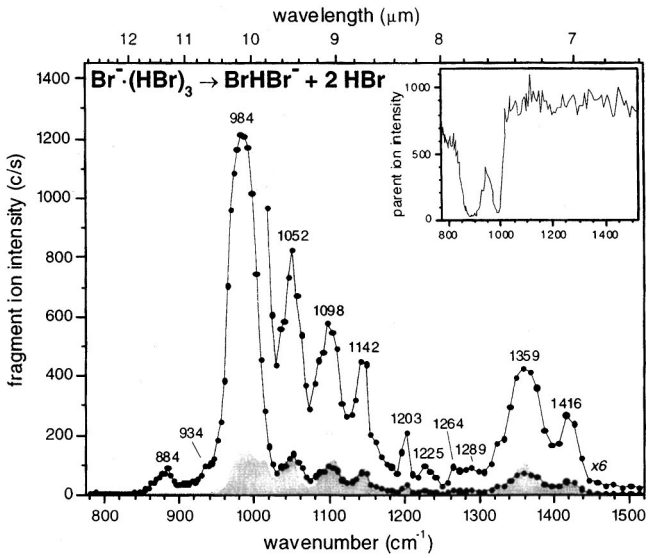

FIG. 4. $BrHBr^-$ fragment ion IRPD spectrum of $Br^-\cdot(HBr)_3$ (solid dots). Gray shaded area shows the $Br^-\cdot(HBr)_2$ IRPD spectrum. Inset shows the corresponding $Br^-\cdot(HBr)_3$ parent depletion spectrum.

tional, overlapping absorption band. Lorentzian fits of these peaks yield widths (FWHM) of 15–21 cm^{-1}, save the peak at 992 cm^{-1}, which is 40 cm^{-1} wide. Lower intensity absorption bands appear in the $BrHBr^-$ fragment ion spectrum at 875, 940, 1205, 1222, 1269, and 1289 cm^{-1}. The fragment ion yield is not equivalent to the depletion signal, mainly due to the optimization of the mass spectrometer for parent ion detection. All observed peak widths are well in excess of the 8–11 cm^{-1} FELIX bandwidth. A background free Br^- fragment ion spectrum (not shown) was also acquired over the same wavelength range, but $<0.2\%$ of the total photoproducts appear as Br^- and no distinct features were observed.

C. $Br^-\cdot(HBr)_3$

The IRPD spectroscopy of $Br^-\cdot(HBr)_3$ was studied in the spectral range from 6 to 16 μm with macropulse energies of 50 mJ and 25 mJ (50% attenuation). At the lower laser power (Fig. 3) the dominant fragmentation products are $Br^-\cdot(HBr)_2+HBr$. Loss of two HBr units leading to the formation of $BrHBr^-$ is also observed, but with considerably less efficiency ($<1\%$ at 888 cm^{-1}). The photofragment yield spectrum for $Br^-\cdot(HBr)_2$ production (solid dots) shows two absorption bands at 888 and 979 cm^{-1}. At 888 cm^{-1} more than 80% of the parent ion signal is depleted (inset of Fig. 3). The width of the intense absorption band is >30 cm^{-1} and may be broadened in part from saturation effects. A constant background of $Br^-\cdot(HBr)_2$ formed by He atom collision induced dissociation in the ion trap is also observed and amounts to $<10\%$ of the fragment ion intensity at the maximum of the main absorption band.

IRPD spectra of $Br^-\cdot(HBr)_3$ taken at a FELIX power of 50 mJ/macropulse are shown in Fig. 4. The parent depletion spectrum differs considerably from the spectrum measured at lower laser power, exhibiting an additional, pronounced minimum at 979 cm^{-1}. Complete saturation of the 884 cm^{-1} transition is effected, with no residual parent ions observed. The single HBr loss spectrum (not shown) looks similar to the one measured at lower laser power (see Fig. 3), but saturation effects significantly broaden the absorption peaks. However, the intensity of the $BrHBr^-+2HBr$ channel (solid dots, Fig. 4) increases significantly at higher power and looks quite different from the single HBr loss channel in Fig. 3. In particular, the $BrHBr^-$ channel is much more intense at 984 cm^{-1} than at 884 cm^{-1}, totally opposite to the intensity distribution in Fig. 3. In addition, a series of much smaller peaks at higher frequency are observed that do not appear in Fig. 3 nor in the parent depletion spectrum in Fig. 4.

The differences between Figs. 3 and 4 arise from two effects. The peak at 984 cm^{-1} nearly coincides with the peak at 992 cm^{-1} in the IRPD spectrum of $Br^-\cdot(HBr)_2$ in Fig. 2. We therefore attribute the 984 cm^{-1} peak in Fig. 4 to a sequential process producing $BrHBr^-$,

$$Br^-\cdot(HBr)_3 \xrightarrow[-HBr]{n\cdot h\nu} Br^-\cdot(HBr)_2 \xrightarrow[-HBr]{n'\cdot h\nu} BrHBr^-, \qquad (2)$$

where $h\nu$ is resonant with a vibrational fundamental in both the $n=2$ and $n=3$ clusters. The small peaks seen in the 1000–1500 cm^{-1} region of the spectrum in Fig. 4 appear at the same locations as peaks in the $Br^-\cdot(HBr)_2$ IRPD spectrum (Fig. 2 and also shown in the gray shaded area of Fig. 4) discussed in the previous section, and these are attributed exclusively to the IRPD of $Br^-\cdot(HBr)_2$ produced by collisional fragmentation of $Br^-\cdot(HBr)_3$ in the ion trap. The intensity of the gray shaded peaks is consistent with the magnitude of $Br^-\cdot(HBr)_2$ fragments observed in the trap in the absence of FELIX excitation, and the absorption cross section of $Br^-\cdot(HBr)_2$.

D. Electronic structure calculations

A sophisticated theoretical treatment of $BrHBr^-$ has been reported recently, in which vibrational energy levels on a multidimensional potential energy surface were

TABLE II. Normal modes, harmonic vibrational frequencies, and oscillator strengths for the C_{2v} ground state of $Br^-\cdot(HBr)_2$ calculated at the B3LYP/aug-cc-pVTZ level of theory.

Symmetry	Frequency (cm^{-1})	Intensity (km/mol)	Description
a_1	1662	1776	symmetric H-atom stretch
b_2	1453	7285	antisymmetric H-atom stretch
a_1	632	<1	in-plane synchronous H-atom wag
a_2	585	0	out-of-plane asynchronous H-atom wag
b_2	568	33	in-plane asynchronous H-atom wag
b_1	567	2	out-of-plane synchronous H-atom wag
a_1	106	13	symmetric Br–Br stretch
b_2	98	123	antisytmmetric Br–Br stretch
a_1	11	≪1	Br–Br bend

determined.[16] However, no calculations of any sort have been done for the larger clusters. Therefore, optimized geometries and vibrational frequencies were calculated for the $Br^-\cdot(HBr)_{2,3}$ clusters at the B3LYP (Ref. 31) level of theory, employing the Dunning correlation consistent split valence triple zeta basis set with diffuse functions (aug-cc-pVTZ) (Refs. 32–34) as packaged in GAUSSIAN 98.[35] Calculated harmonic vibrational frequencies, IR intensities, and approximate mode descriptions for both clusters are listed in Tables II and III. The minimum energy structures found are shown in Fig. 5. $Br^-\cdot(HBr)_2$ exhibits a C_{2v} minimum energy structure with two HBr ligands complexed to a central Br^-. Addition of a third HBr ligand yields a C_{3v} minimum energy structure for $Br^-\cdot(HBr)_3$.

The inner HBr bond lengths for the $n=2$ and 3 clusters were found to be 2.03 and 2.16 Å and the terminal HBr bond lengths were calculated to be 1.53 and 1.49 Å. The terminal HBr bond lengths in the $n=2$ and 3 clusters are nearer the unperturbed HBr bond length of 1.4144 Å (Ref. 36) than the previously calculated[16] HBr bond lengths of 1.73 Å in $BrHBr^-$. The Br–Br distances increase by ~0.1 Å per additional HBr ligand. The calculations predict that the addition of even a single HBr to $BrHBr^-$ destroys the symmetrical hydrogen bond in the bihalide; the two larger cluster ions are

TABLE III. Normal modes, harmonic vibrational frequencies, and oscillator strengths for the C_{3v} ground state of $Br^-\cdot(HBr)_3$ calculated at the B3LYP/aug-cc-pVTZ level of theory.

Symmetry	Frequency (cm^{-1})	Intensity (km/mol)	Description
a_1	1981	480	symmetric H atom stretch
e	1807	4669	antisymmetric H atom stretch
e			
e	559	≪1	H atom wag
a_1	527	2	H atom wag
a_2	514	0	H atom wag
e	512	1	H atom wag
e	101	46	antisymmetric HBr stretch
a_1	90	2	symmetric HBr stretch
e	12	≪1	HBr wag
a_1	11	≪1	intramolecular umbrella

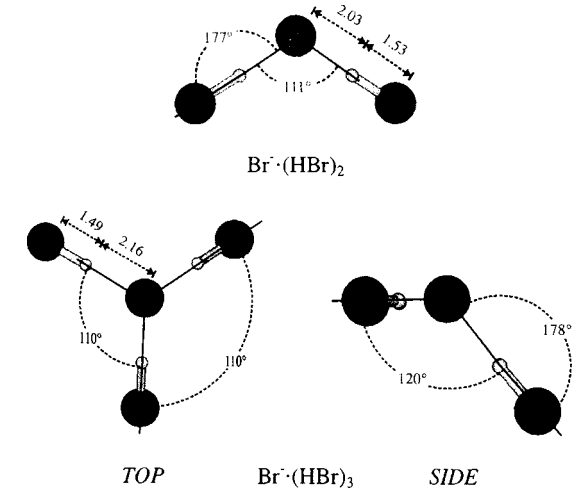

FIG. 5. Structures of $Br^-\cdot(HBr)_3$ (above) and $Br^-(HBr)_2$ (below) calculated at the B3LYP//aug-cc-pVTZ level of theory. Upper panel shows bond lengths and angles for the C_{2v} $Br^-\cdot(HBr)_2$ complex. Lower panel shows top and side views of the C_{3v} $Br^-\cdot(HBr)_3$ complex ion. H–Br–H and Br–Br–Br bond angles are indicated in the top view, along with inner and outer H–Br bond lengths (Å). Side view shows slight deviation from linearity in the Br–H–Br bond, and also illustrates the 120° dihedral of the third HBr ligand.

better represented as HBr ligands complexed to a central bromide ion. The effect of solvation on binary hydrogen bonds in negatively charged species was recently probed by Robertson *et al.* in an IR study of $Cl^-(H_2O)(CCl_4)_n$ clusters, where addition of a single CCl_4 molecule was shown to perturb the Cl–H–O bond length.[37]

These trends are reflected in the calculated frequencies and intensities in Tables II and III, according to which the IR spectroscopy of the $n=2$ and $n=3$ clusters should be dominated by two modes representing symmetric and antisymmetric linear combinations of HBr stretches. The calculated frequencies for these modes lie between the $BrHBr^-$ antisymmetric stretch, 753 cm^{-1}, and the HBr fundamental at 2559 cm^{-1}, indicating significant and increasing perturbation of the hydrogen bond in $BrHBr^-$ by the additional HBr molecules.

The zero point corrected binding energies of a single HBr ligand to $Br^-\cdot(HBr)_2$ and $Br^-\cdot(HBr)_3$ were calculated to be 2963 and 3918 cm^{-1}. The HBr binding energy of $BrHBr^-$ calculated by the same method was 7582 cm^{-1}, which agrees reasonably well with the experimental binding energy of 7480 cm^{-1} reported by Caldwell *et al.*[4]

The C_{2v} structure calculated for $Br^-\cdot(HBr)_2$ is consistent with past experimental and theoretical work on $Cl^-(HCl)_2$ and $F^-\cdot(HF)_2$ which showed similar structures for these clusters.[38–44] Likewise, the C_{3v} structure calculated for $Br^-\cdot(HBr)_3$ confirms the trend observed in previously calculated structures for $F^-\cdot(HF)_3$ and $Cl^-\cdot(HCl)_3$ which predicted a geometry change from D_{3h} to C_{3v} in the transition from fluorine to chlorine.[38,39,42]

IV. DISCUSSION

The observed absorption band of $BrHBr^-$ at 1558 cm^{-1} is assigned to the overtone of the ν_3 absorption band previ-

ously observed at 728 and 753 cm^{-1} in matrix IR studies.[8,12] The high negative anharmonicity implied by this assignment is consistent with the calculations by Del Bene and Jordan,[16] who find a substantial negative anharmonicity for the ν_3 mode in FHF^-, $ClHCl^-$, and $BrHBr^-$.

For $Br^-\cdot(HBr)_2$, using the calculated results in Table II as a guide, the experimental peaks at 1359 and 1420 cm^{-1} are closest in frequency to the calculated harmonic frequencies of 1453 and 1662 cm^{-1} for the b_2 and a_1 antisymmetric and symmetric HBr stretches, and the experimental and calculated relative intensities of the two peaks agree reasonably well. The calculated frequencies for the corresponding modes in $Br^-\cdot(HBr)_3$ are higher and would be out of range of the instrument due to the ZnSe windows. One would then assign the peaks around 1000 cm^{-1} for the two clusters to combination bands of the various bending modes for which the calculated fundamentals lie between 500–600 cm^{-1}. However, this assignment is problematic because the calculated IR intensities for the bend fundamentals are several orders of magnitude lower than for the HBr stretches, whereas in the experimental spectrum for $Br^-(HBr)_2$, the peaks around 1000 cm^{-1} are more intense than the 1359/1416 cm^{-1} doublet.

These considerations lead one to question the reliability of the calculated harmonic frequencies for the asymmetric hydrogen bonds in these clusters. Indeed, in a theoretical study $BrHI^-$, a prototypical asymmetric bihalide, by Morokuma and co-workers,[45] the harmonic frequency of the ν_3 mode obtained was found to be 1779 cm^{-1}, substantially higher than the 1267 cm^{-1} frequency obtained by constructing a full three-dimensional surface for $BrHI^-$ and calculating the eigenvalues, and higher still than either of the two reported matrix IR spectroscopy values, 666 and 920 cm^{-1}.[6] Additionally, the harmonic antisymmetric H-atom stretch of the asymmetric $F^-\cdot(HF)_2$ complex was calculated at 2364 cm^{-1},[40] while experimental work placed the frequency at 1815 cm^{-1}.[44] As an alternate assignment, the bands at 992 and 1048 cm^{-1} for $Br^-\cdot(HBr)_2$ and 888 and 979 cm^{-1} for $Br^-\cdot(HBr)_3$ could be the fundamentals of the two H-atom stretch vibrations. The higher frequency peaks in the $Br^-\cdot(HBr)_2$ spectrum then result from combination bands; comparison with Table II suggests the likeliest candidates are the b_2 H-atom wag and antisymmetric Br–Br stretch modes, with calculated frequencies of 568 and 98 cm^{-1}, respectively, and small but nonzero IR intensities. While neither set of assignments is wholly satisfactory, both place the antisymmetric HBr stretch at a considerably higher frequency than the ν_3 fundamental in $BrHBr^-$, providing experimental evidence for destruction of the symmetric hydrogen bond and localization of the H atom in the larger clusters.

Comparison of the three ions studied here suggests that $BrHBr^-$ lies in a different regime with respect to multiphoton absorption and dissociation than the two larger clusters. In the generally accepted picture of multiphoton absorption and dissociation within the low field approximation (the maximum photon flux at the interaction region is on the order of 10^{11} W/cm^2),[46,47] absorption of the first few photons occurs within the ''discrete'' regime, in which the photons resonantly excite a particular vibrational mode of a molecule. Higher excitation accesses the ''quasicontinuum'' regime in which the density of states is so high that the vibrational energy is rapidly randomized among all vibrational modes of the molecule; the transition between the two regimes depends on the vibrational density of states and the strengths of the interactions between vibrational modes. The molecule continues to absorb photons until the dissociation rate exceeds the up-pumping rate.

In $BrHBr^-$, the ν_3 mode exhibits significant negative anharmonicity; the fundamental frequency is 730–750 cm^{-1}, but the first overtone is centered at 1558 cm^{-1}. Hence, the absence of the fundamental and low dissociation yield for $BrHBr^-$ for the overtone indicates that the discrete regime acts as an anharmonic bottleneck, with one-color excitation unable to resonantly excite both the 1–0 and 2–1 transitions. On the other hand, observation of the overtone transition suggests the density of states near 3000 cm^{-1} is sufficiently high for absorption of the second (and subsequent) photon to occur under the conditions of our experiment. In addition, ~10 collisions with the He buffer gas occur during the 5 μs duration of each macropulse, resulting in additional state mixing that can facilitate multiphoton absorption.

In the $Br^-\cdot(HBr)_{2,3}$ clusters, the additional HBr ligands raises the vibrational density of states relative to $BrHBr^-$, and based on the calculations in Sec. III, the dissociation energies are lower. The breakdown of the harmonic approximation for the description of the H-atom stretch modes also hints at a considerable coupling of the vibrational modes. All three effects favor multiphoton absorption and dissociation, consistent with the much higher signals seen for the two larger clusters. Hence, these clusters behave more like the cation clusters previously studied with FELIX.[28,48]

The results presented here show that IRPD studies with FELIX can access the vibrational spectroscopy of anions spanning a wide size range, and in particular can be applied to anions with as few as three atoms. It is therefore an ideal method for observing the size-dependence of the vibrational spectroscopy of anion clusters over an extended frequency range that has previously been inaccessible. In the case of the hydrogen bonded clusters studied here, the inclusion of anharmonic effects is a prerequisite for an adequate theoretical description of the IR spectra of these species.

ACKNOWLEDGMENTS

This work is funded by the Sonderforschungsbereich 546 and the Ph.D. Graduate Study Program 788 of the Deutsche Forschungsgemeinschaft. United States Air Force Office of Scientific Research Grant No. F49620-00-1-0018 provided support for N.L.P. The authors gratefully acknowledge the support of the *Stichting voor Fundamenteel Onderzoek der Materie* (FOM) in providing the required beam time on FELIX and highly appreciate the skillful assistance of the FELIX staff, in particular Dr. A. F. G. van der Meer. This work was supported in part under the ''Access to research infrastructure action of the Improving Human Potential Program'' of the European Community. The authors would like to thank Professor Dr. W. J. Buma of the University of Amsterdam for the loan of HBr gas.

[1] G. C. Pimentel and A. L. McClellan, *The Hydrogen Bond* (Freeman, San Francisco, 1960).
[2] U. Buck and F. Huisken, Chem. Rev. **100**, 3863 (2000).
[3] F. N. Keutsch and R. J. Saykally, PNAS **98**, 10533 (2001).
[4] G. Caldwell and P. Kebarle, Can. J. Chem. **63**, 1399 (1985).
[5] J. Emsley, Chem. Soc. Rev. **9**, 91 (1980).
[6] B. S. Ault, Acc. Chem. Res. **15**, 103 (1982).
[7] V. Bondybey, G. C. Pimentel, and P. N. Noble, J. Chem. Phys. **55**, 540 (1971).
[8] D. E. Milligan and M. E. Jacox, J. Chem. Phys. **55**, 2550 (1971).
[9] K. Kawaguchi and E. Hirota, J. Chem. Phys. **84**, 2953 (1986).
[10] K. Kawaguchi and E. Hirota, J. Chem. Phys. **87**, 6838 (1987).
[11] K. Kawaguchi, J. Chem. Phys. **88**, 4186 (1988).
[12] C. L. Lugez, M. E. Jacox, and W. E. Thompson, J. Chem. Phys. **105**, 3901 (1996).
[13] C. L. Janssen, W. D. Allen, H. F. Schaefer, and J. M. Bowman, Chem. Phys. Lett. **131**, 352 (1986).
[14] A. B. Sannigrahi and S. D. Peyerimhoff, Chem. Phys. Lett. **148**, 197 (1988).
[15] S. Ikuta, T. Saitoh, and O. Nomura, J. Chem. Phys. **93**, 2530 (1990).
[16] J. E. Del Bene and M. J. T. Jordan, Spectrochim. Acta, Part A **55**, 719 (1999).
[17] S. E. Bradforth, A. Weaver, D. W. Arnold, R. B. Metz, and D. M. Neumark, J. Chem. Phys. **92**, 7205 (1990).
[18] R. B. Metz, A. Weaver, S. E. Bradforth, T. N. Kitsopoulos, and D. M. Neumark, J. Phys. Chem. **94**, 1377 (1990).
[19] M. S. Johnson, K. T. Kuwata, C. K. Wong, and M. Okumura, Chem. Phys. Lett. **260**, 551 (1996).
[20] C. G. Bailey, J. Kim, C. E. H. Dessent, and M. A. Johnson, Chem. Phys. Lett. **269**, 122 (1997).
[21] P. Ayotte, G. H. Weddle, J. Kim, and M. A. Johnson, Chem. Phys. **239**, 485 (1998).
[22] O. M. Cabarcos, C. J. Weinheimer, J. M. Lisy, and S. S. Xantheas, J. Chem. Phys. **110**, 5 (1999).
[23] P. S. Weiser, D. A. Wild, and E. J. Bieske, J. Chem. Phys. **110**, 9443 (1999).
[24] H. Piest, G. von Helden, and G. Meijer, J. Chem. Phys. **110**, 2010 (1999).
[25] J. Oomens, A. J. A. van Roij, G. Meijer, and G. von Helden, Astrophys. J. **542**, 404 (2000).
[26] J. Oomens, B. G. Sartakov, A. G. G. M. Tielens, G. Meijer, and G. von Helden, Astrophys. J. Lett. **560**, L99 (2001).
[27] J. Oomens, G. Meijer, and G. von Helden, J. Phys. Chem. A **105**, 8302 (2001).
[28] K. R. Asmis, M. Brummer, C. Kaposta, G. Santambrogio, G. von Helden, G. Meijer, K. Rademann, and L. Woste, Phys. Chem. Chem. Phys. **4**, 1101 (2002).
[29] D. Oepts, A. F. G. Vandermeer, and P. W. Vanamersfoort, Infrared Phys. Technol. **36**, 297 (1995).
[30] M. Rasanen, J. Seetula, and H. Kunttu, J. Chem. Phys. **98**, 3914 (1993).
[31] A. D. Becke, J. Chem. Phys. **98**, 5648 (1993).
[32] T. H. Dunning, J. Chem. Phys. **90**, 1007 (1989).
[33] R. A. Kendall, T. H. Dunning, and R. J. Harrison, J. Chem. Phys. **96**, 6796 (1992).
[34] A. K. Wilson, D. E. Woon, K. A. Peterson, and T. H. Dunning, J. Chem. Phys. **110**, 7667 (1999).
[35] M. J. Frisch, G. W. Trucks, H. B. Schlegel *et al.*, GAUSSIAN 98, Gaussian, Inc., Pittsburgh, PA, 1998.
[36] D. H. Rank, U. Fink, and T. A. Wiggins, J. Mol. Spectrosc. **18**, 170 (1965).
[37] W. H. Robertson, G. H. Weddle, J. A. Kelley, and M. A. Johnson, J. Phys. Chem. A **106**, 1205 (2002).
[38] W. D. Chandler, K. E. Johnson, and J. L. E. Campbell, Inorg. Chem. **34**, 4943 (1995).
[39] W. D. Chandler, K. E. Johnson, B. D. Fahlman, and J. L. E. Campbell, Inorg. Chem. **36**, 776 (1997).
[40] V. P. Bulychev, G. S. Denisov, H. H. Limbach, and R. M. Shukailov, Opt. Spectrosc. **90**, 356 (2001).
[41] J. E. Del Bene, M. J. T. Jordan, S. A. Perera, and R. J. Bartlett, J. Phys. Chem. A **105**, 8399 (2001).
[42] K. N. Rankin, W. D. Chandler, and K. E. Johnson, Can. J. Chem. **77**, 1599 (1999).
[43] T. von Rosenvinge, M. Parrinello, and M. L. Klein, J. Chem. Phys. **107**, 8012 (1997).
[44] R. D. Hunt and L. Andrews, J. Chem. Phys. **87**, 6819 (1987).
[45] A. Kaledin, S. Skokov, J. M. Bowman, and K. Morokuma, J. Chem. Phys. **113**, 9479 (2000).
[46] A. S. Sudbo, P. A. Schulz, E. R. Grant, Y. R. Shen, and Y. T. Lee, J. Chem. Phys. **70**, 912 (1979).
[47] M. Quack, Ber. Bunsenges. Phys. Chem. **83**, 757 (1979).
[48] D. Heijnsbergen, M. A. Duncan, G. Meijer, and G. von Helden, Chem. Phys. Lett. **349**, 220 (2001).